



**HAL**  
open science

# Energy-Efficient Routing, Power Control and Energy Clustering for Energy Harvesting-Enabled Spectrum Sharing IoT Sensor Networks ★

Derek Kwaku Pobi Asiedu, Kyoung-Jae Lee, Ji-Hoon Yun

## ► To cite this version:

Derek Kwaku Pobi Asiedu, Kyoung-Jae Lee, Ji-Hoon Yun. Energy-Efficient Routing, Power Control and Energy Clustering for Energy Harvesting-Enabled Spectrum Sharing IoT Sensor Networks ★. Internet of Things, 2024, 25, pp.101122. 10.1016/j.iot.2024.101122 . hal-04599826

**HAL Id: hal-04599826**

**<https://imt-atlantique.hal.science/hal-04599826>**

Submitted on 4 Jun 2024

**HAL** is a multi-disciplinary open access archive for the deposit and dissemination of scientific research documents, whether they are published or not. The documents may come from teaching and research institutions in France or abroad, or from public or private research centers.

L'archive ouverte pluridisciplinaire **HAL**, est destinée au dépôt et à la diffusion de documents scientifiques de niveau recherche, publiés ou non, émanant des établissements d'enseignement et de recherche français ou étrangers, des laboratoires publics ou privés.

# Energy-Efficient Routing, Power Control and Energy Clustering for Energy Harvesting-Enabled Spectrum Sharing IoT Sensor Networks<sup>\*</sup>

Derek Kwaku Pobi Asiedu<sup>a</sup>, Kyoung-Jae Lee<sup>b</sup>, Ji-Hoon Yun<sup>a,\*</sup>

<sup>a</sup>*Department of Electrical and Information Engineering, Seoul National University of Science and Technology, 232 Gongneung-ro, Nowon-gu, Seoul, 01811, Seoul, Korea*

<sup>b</sup>*Department of Electronic Engineering, Hanbat National University, 34158 125, Dongseo-daero, Yuseong-gu, Daejeon, 34158, Chungcheongnam-do, Korea*

---

## Abstract

We investigate a spectrum sharing system that enables energy harvesting from distributed multi-antenna energy transmitter devices for primary dual-band device-to-device networks and secondary dual-band wireless sensor networks (WSNs), incorporating a multi-stage rectenna energy harvesting circuit model. We formulate a new multi-hop routing problem for network energy efficiency maximization of this system, which involves the interconnected tasks of WSN routing, controlling the transmit power of sensor nodes, and energy transmitter clustering, taking into account interference, power budget and rate constraints. To tackle these interconnected tasks effectively, we propose an integrated solution that includes both centralized and distributed routing schemes. Furthermore, the solution incorporates energy transmitter clustering schemes based on harvested power and channel gain. We provide an analysis of the computation complexity and signaling overhead for the proposed solution. Our simulation results demonstrate that the proposed routing and clustering schemes outperform their respective benchmark schemes, achieving significant performance gains.

*Keywords:* wireless power transfer, energy harvesting, clustering, energy efficiency, multi-hop routing.

---

<sup>\*</sup>Funding: This study was financially supported by Seoul National University of Science and Technology.

<sup>\*</sup>Corresponding author.

*Email address:* [jhyun@seoultech.ac.kr](mailto:jhyun@seoultech.ac.kr) (Ji-Hoon Yun)

---

## 1. Introduction

In recent decades, Internet of Things (IoT) sensor networks have gained significant attention due to their wide-ranging applications in multi-scale environmental monitoring for IoT, such as smart farms, smart factories, and public safety networks [1, 2, 3]. Multi-hop networking has emerged as a popular and efficient method for collecting sensor data across vast geographical areas in these applications. Considering the limited availability of spectrum resources, IoT sensor networks can effectively utilize multi-hop networking to coexist and share the spectrum with primary user-device networks, thereby enhancing overall network performance and spectrum efficiency [1, 2]. In addition, energy harvesting (EH) through radio frequency (RF) wireless power transfer (WPT) has been identified as a promising and sustainable strategy to extend the operational life of IoT sensor networks, offering a means to replenish the energy of sensor nodes and address the challenge of limited battery capacity.

Existing research on EH-IoT sensor networks, also referred to as EH-wireless sensor networks (EH-WSNs), has primarily focused on routing with objectives such as minimizing transmit power [4, 2], optimizing two-hop energy efficiency [5, 6, 7] or maximizing network capacity [8, 9]. While these specific performance metrics for routing are valuable in their respective areas, they may not comprehensively address the challenges associated with energy constraints in EH-WSNs. An essential metric that encapsulates these challenges is the multi-hop network energy efficiency (NEE), which is defined as the ratio of system rate to total power consumption. Recent studies have explored spectrum sharing of WSNs as secondary users, also known as EH-cognitive radio sensor networks (EH-CRSNs). These studies have focused on developing clustering mechanisms for sensors nodes (SNs) [10], radio resource management [11, 12, 13], and routing protocols [14, 15, 16, 17]. Additionally, prior research has investigated distributed energy transmitter (ET) configurations in homogeneous networks [18, 19]. However, there is still a research gap in understanding and developing ET configurations within the context of energy-efficient routing for spectrum sharing networks that consist of heterogeneous network layers, including a secondary WSN layer.

This paper presents a spectrum sharing system comprising three network layers: a dual-band licensed primary EH-aided device-to-device (D2D) com-

munication network layer, a single-band distributed ET layer, and a dual-band secondary EH-aided WSN layer. We then address the challenge of optimizing NEE by formulating a new multi-hop routing problem within this system. This problem involves tasks such as WSN routing, controlling the transmit power of SNs, and ET clustering. These tasks are interconnected and operate under various constraints, including interference considerations for the primary D2D network, as well as power budget and minimum rate constraints for SNs. It is noted that existing research, including studies on EH-CRSNs, has not considered these interconnected task problems and crucial interference management aspects.

We propose a solution that addresses these interconnected problems associated with the three-layer spectrum sharing network system for NEE optimization. This solution employs a main loop to determine a route for a given source SN to the gateway node, which is implemented in both centralized and distributed manners. Within this loop, for each candidate routing SN, an ET cluster is determined using schemes based on harvested power and channel gain. Following this, the corresponding power budget for a multi-stage rectifier EH circuitry is obtained. Within this budget, a transmit power optimization problem is solved under primary network (PN) interference constraints, utilizing the Dinkelbach dual decomposition method. Ultimately, the SN with the highest NEE is selected as the next routing SN, and this process is repeated until the gateway node is reached. We provide an in-depth analysis of the computation complexity and signaling overhead for the proposed solution.

We evaluate the effectiveness of the proposed solution and accompanying schemes by comparing them to benchmark methods, which include distance- and channel-based routing schemes and a naive all-to-all ET-to-SN clustering. The simulation results show that our proposed solution surpasses the benchmarks in terms of NEE and EH performance.

The main contributions of our work are summarized as follows:

- *New system and problem:* We introduce a new spectrum sharing system that operates between a primary D2D layer and a secondary WSN utilizing dual frequency bands for EH from an ET layer. A new NEE optimization problem for this system requiring WSN routing, transmit power control of SNs, and ET clustering, while taking into account interference constraints and power budgets, is formulated.
- *Holistic solution for NEE:* We develop a new solution that holistically

addresses the multi-layered challenges inherent in the proposed spectrum sharing system, which is available in two distinct versions: centralized and distributed, each offering unique performance characteristics and overhead considerations. Furthermore, this solution is paired with an advanced multi-stage EH model, which has not been considered in previous EE routing studies in the literature.

- *Comprehensive analysis and evaluation:* We conduct a thorough analysis of the computational complexity and signaling overhead associated with our proposed solution, considering various associated schemes. Extensive simulation work demonstrates the performance advantages of our solution over various benchmarks, under a range of network conditions.

The rest of the paper is organized as follows. Recent studies related to energy-efficient routing are reviewed and discussed in Section 2. The system model is comprehensively presented in Section 3. Section 4 presents the problem formulation. In Section 5, we describe the proposed solution. We provide an analysis of computation complexity and signaling overhead in Section 6. The simulation results are presented and discussed in Section 7. Finally, Section 8 concludes the paper.

*Notations:* The notations  $\|\cdot\|$  and  $|\cdot|$  represent the  $l_2$ -norm and absolute values, respectively. The symbol  $\Re\{x\}$  denotes the real part of a complex number  $x$ . Lowercase bold letters are used to represent vectors. We employ the notation “ $\triangleq$ ” to indicate “defined as equal to”. Tables 1 and 2 list the abbreviations and notations, respectively, that are frequently used in the paper.

## 2. Related works

In the work of Tran et al. [20], a routing protocol for WSNs was introduced, focusing on energy-efficient multi-hop WSN clusters. The authors determined the weighting factor by calculating the negative difference between the residual energy of the transmitting SN and the energy consumed for packet transmission to the receiving SN. He et al. [21] explored the use of power splitting techniques for simultaneous wireless information and power transfer (SWIPT) in WSNs, specifically focusing on making energy-efficient routing decisions. The inter-node communication in their approach involved either using the SN’s battery power to transmit the information

Table 1: List of frequently used abbreviations.

Abbreviation	Definition
CC (HC)	Channel gain (harvested power)-based clustering
CRM (DRM)	Centralized (distributed) routing method
CLCGRM (DLCGRM)	Centralized (distributed) maximum inter-node channel gain routing method
CSDRM (DSDRM)	Centralized (distributed) minimum inter-node distance routing method
EHN	Energy harvesting node
ET	Energy transmitter
MRT	Maximum ratio transmission
NEE	Network energy efficiency
PL (SL)	Primary (secondary) link
PN (SN)	Primary network (sensor node)
PT (ST)	Primary (secondary) transmitter
PR (SR)	Primary (secondary) receiver

signal or utilizing harvested energy from the received signal for transmission. They defined a routing metric based on the minimum transmit energy required to satisfy an inter-node rate constraint. Hao et al. [22] proposed an energy-efficient routing protocol based on a greedy strategy, considering the relationship between energy state and data buffer constraints. Han et al. [23] introduced an adaptive hierarchical-clustering-based routing protocol for EH-WSNs. Their goal was to achieve uninterrupted coverage of the target region through distributed adjustment of data transmission. In the work of Kim et al. [24], a routing mechanism was proposed to balance the energy consumption among all SNs and prolong the WSN lifetime. They assigned a score value to each SN along a path, which was determined by combining evaluation metrics. Subramani et al. [25] proposed a clustering-based routing protocol specifically designed for underwater WSNs. The unique challenges in underwater environments, such as underwater currents, low bandwidth, high water pressure, propagation delay, and error probability, necessitated the development of a specialized protocol.

Existing research on EH-CRSNs has primarily focused on resource allocation, management, and node clustering. In the context of node clustering, Aslam et al. [10] proposed a two-level node classification algorithm based on

Table 2: Summary of notations.

Symbol	Definition
$\mathcal{P}, \mathcal{S}, \mathcal{E}$	The sets of PLs, SNs and ETs, respectively
$\mathcal{S}_k$	The set of neighboring SNs for $u_k$ ( $k$ th routing node)
$M^{PL}, M^{SN},$	The numbers of PLs, SNs and ETs, respectively
$f_I, f_p$	Information and power transmission frequency bands, respectively
$K$	Number of routing nodes for a route
$N^{ET}$	Number of ET antennas
$h_{l=(u,v)}^{IT}$	Channel for a link $l$ between SNs $u$ and $v$
$h_{r,v}^{PT}$	Channel between PT $r$ and SN $v$
$\mathbf{h}_{m,x}^{ET}$	Channel between ET $x$ and EHN $m$
$s^z, \psi^z$	Amplitude and phase for node $z$ , respectively
$\Re\{\cdot\}, \Im\{\cdot\}$	Real and imaginary components, respectively
$l_T, l_R$	Transmitter and receiver nodes of link $l$ , respectively
$\mathbf{r}_{u,v}$	Route from SN $u$ to SN $v$
$\Gamma_{u,v}$	Energy efficiency for a route from SN $u$ to SN $v$
$P_v^{IT}, P_{out,v}^{DC}, \hat{P}_v^{use},$	Transmit, receive circuitry and harvested powers of SN $v$ , respectively
$B_v$	Remaining batter power
$Q_{l_T}$	Interference threshold associated with link $l$
$R_l$	Data rate of link $l$
$R_{TH,l}$	Minimum rate threshold for link $l$
$R_{ant,m}$	EH antenna impedance of EHN $m$
$R_{Lod,m}$	EH circuit output load resistance
$G_m$	Number of EH circuitry stages
$\eta_m, V_{T,m}$	Ideality factor and thermal voltage of EH circuitry, respectively
$\mathcal{Q}$	Set of selected routing SNs for a current route

K-means clustering, taking into account node energy and channel availability. In their work, Aslam et al. [11] proposed an energy and channel allocation strategy to address the intra-cluster energy and channel management problem. Wang et al. [12] introduced intelligent reflecting surface (IRS)-aided CRSNs and developed a shared reflection coefficient matrix-based EH

scheme to enhance energy harvesting performance. Liu et al. [13] proposed a spectrum lease mode-based subchannel and resource joint allocation strategy, which considered the outage probability to ensure network robustness. However, these mentioned works did not specifically address the multi-hop routing problem in EH-CRSNs.

Several multi-hop routing protocols have been developed in recent studies on EH-CRSNs. In the work of Wang et al. [14], a multihop clustering routing protocol was proposed to address the effective data transmission problem. They also derived the optimal number of clusters with the objective of minimizing total energy consumption for data communication. In [15], the authors developed a distributed energy balance-oriented uneven clustering routing protocol, considering both the energy consumption of control information exchange and data transmission. To improve network surveillance capability and network lifetime, [16] proposed a weighted energy consumption minimization-based uneven clustering routing protocol. The authors of [17] developed an imperfect spectrum sensing-based multi-hop clustering routing protocol to mitigate the impact of imperfect spectrum sensing on network performance. However, it is important to note that existing multi-hop routing protocols for EH-CRSNs have yet to adequately consider interference constraints of PNs and power control for secondary SNs.

### 3. System Model

Fig. 1 illustrates the considered spectrum sharing network system, which is composed of three network layers: (a) a PN that consists of a set  $\mathcal{P}$  of D2D primary links (PLs), each with a dual-antenna, dual-band EH primary transmitter (PT) and receiver (PR); (b) a WSN consisting of a set  $\mathcal{S}$  of dual-antenna dual-band EH SNs, including a gateway node; and (c) a set  $\mathcal{E}$  of multi-antenna distributed ETs. The sets  $\mathcal{P}$ ,  $\mathcal{S}$ , and  $\mathcal{E}$  have cardinalities  $M^{PL}$ ,  $M^{SN}$ , and  $M^{ET}$ , respectively. Each PT transmits data to its nearby PR, while the SNs send environmental sensing data to the gateway node, along a multi-hop SN route. Each EH node (EHN)  $m$  (either PT, PR or SN) is associated with a cluster of ETs, denoted by  $\mathcal{E}_m (\subseteq \mathcal{E})$ , from which the EHN harvests energy. The EHNs transmit and receive information (data) signals and receive power signals over  $f_I$  and  $f_P$  frequency bands, respectively, utilizing their dual-antenna dual-band configuration like [26, 27, 28]. This implies that primary and secondary data transmissions may interfere with each other, but the energy transmissions from the ETs do not cause

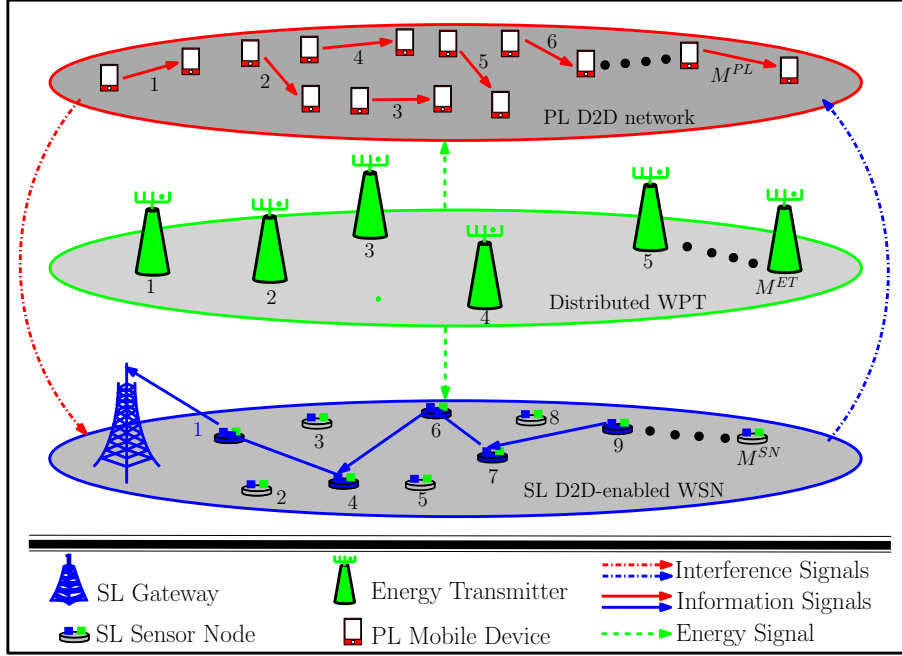


Figure 1: Proposed wireless powered spectrum sharing network system.

interference to data signals. Each ET  $x \in \mathcal{E}$  is equipped with  $N_x^{ET}$  antennas. A route from SN  $u$  to SN  $v$ , ( $u, v \in \mathcal{S}$ ) is represented by a sequence of directional links, denoted as  $\mathbf{r}_{u,v} = (l_0, \dots, l_{K-1})$ , where  $K$  is the number of hops in the route. We express a link  $l_k$  as a pair of the transmitter  $u_k$  and the receiver  $u_{k+1}$ , i.e.,  $l_k = (u_k, u_{k+1})$ ;  $u_0$  denotes the source SN of a route. The transmitter and receiver nodes of link  $l$  are also denoted by  $l_T$  and  $l_R$ , respectively.

For a link  $l = (u, v)$ , the signal received by SN  $v$  in the frequency band  $f_I$  at time  $t$  is given as

$$\begin{aligned}
 y_v^{IR}(t) = & \underbrace{w_v^{BB}(t)}_{\text{Noise}} + \underbrace{\Re\{h_l^{IT} s_u^{IT} e^{j\psi_u^{IT}} e^{j2\pi f_I t}\}}_{\text{Information signal from SN } u} \\
 & + \underbrace{\Re\left\{\sum_{r=l_T, l \in \mathcal{P}} h_{r,v}^{PT} s_r^{PT} e^{j\psi_r^{PT}} e^{j2\pi f_I t}\right\}}_{\text{Interference signals from } \{\text{PT } r\}_{r=l_T, l \in \mathcal{P}}}, \quad (1)
 \end{aligned}$$

where  $(s_u^{IT}, \psi_u^{IT})$  and  $(s_r^{PT}, \psi_r^{PT})$  are the (amplitude and phase) variable sets of SN  $u$  and PT  $r$  signals, respectively, with  $r = l_T, l \in \mathcal{P}$ ;  $h_l^{IT}$  and

$h_{r,v}^{PT}$  are the channel frequency responses of link  $l$  and the  $r$ -to- $v$  path, respectively. The power constraints for SN  $u$  and PT  $r$  are  $|s_u^{IT}|^2 = P_u^{IT}$  and  $|s_r^{PT}|^2 = P_r^{PT}$ , respectively. Assuming independent and identically distributed random variables for channel input and discrete memoryless channels, the output of the analog-to-digital conversion is obtained as  $\tilde{y}_v^{IR} = h_l^{IT} s_u^{IT} + \sum_{r=1}^{M^{PL}} h_{r,v}^{PT} s_r^{PT} + w_v^{BB}$ , where  $w_v^{BB}$  is a Gaussian random variable representing the baseband noise floor with variance  $\sigma^2$ . Applying Shannon's capacity theorem, the rate of link  $l$  with bandwidth  $W$  is calculated as  $R_l = W \log_2 \left( 1 + \frac{|h_l^{IT}|^2 P_u^{IT}}{\sum_{r=l_T, l \in \mathcal{P}} |h_{r,v}^{PT}|^2 P_r^{PT} + \sigma^2} \right)$ .

The signal received by EHN  $m$  from  $\mathcal{E}_m$  is given by

$$y_m^{EH}(t) = \sum_{x \in \mathcal{E}_m} y_{m,x}^{EH}(t) = \Re \left\{ \sum_{x \in \mathcal{E}_m} \mathbf{h}_{m,x}^{ET} \mathbf{s}_{x,m}^{ET} e^{j2\pi f_P t} \right\} \quad (2)$$

where  $y_{m,x}^{EH}$  is the power signal from ET  $x$ ,  $\mathbf{h}_{m,x}^{ET}$  and  $\mathbf{s}_{x,m}^{ET}$  are the channel frequency response and beamforming signal vectors of ET  $x$ 's signal operating with maximum emission power  $P_x^{ET}$ . When EHN  $m$ 's antenna impedance is  $R_{ant,m}$ , its EH circuit RF(AC)-to-DC converter produces the input voltage of  $V_{in,m}(t) = y_m^{EH}(t) \sqrt{R_{ant,m}}$ . Let  $V_{out,m,x}$  be the output voltage harvested from the signal of ET  $x (x \in \mathcal{E}_m)$ . Then, the final DC output voltage  $V_{out,m}$  is given as  $\sum_{x \in \mathcal{E}_m} V_{out,m,x}$ . We assume a  $G_m$ -stage EH circuit, for which the DC output voltage component for  $y_{m,x}^{ET}(t)$  is obtained as  $V_{out,m,x} = \frac{G_m R_{ant,m} f_{LPF}(y_{m,x}^{ET}(t))^2}{\eta_m V_{T,m}} + \frac{1}{12} \frac{G_m R_{ant,m}^2 f_{LPF}(y_{m,x}^{ET}(t))^4}{\eta_m^3 V_{T,m}^3}$ , where  $f_{LPF}()$ ,  $\eta_m$ , and  $V_{T,m}$  are an ideality factor, a low pass filter, and thermal voltage, respectively [29]. When the EH circuit output resistance load is  $R_{Lod,m}$ , the power harvested by EHN  $m$  is obtained as  $P_{out,m}^{DC} = V_{out,m}^2 / R_{Lod,m}$ .

#### 4. Problem Formulation

We define the NEE as the ratio of the sum-rate of the links in a route to the total power consumption of those links. For a route  $\mathbf{r}_{u,v}$ ,  $u, v \in \mathcal{S}$ , this is expressed as

$$\Gamma_{u,v} \triangleq \frac{\sum_{l \in \mathbf{r}_{u,v}} R_l}{\sum_{l \in \mathbf{r}_{u,v}} (P_{l_T}^{IT} + \hat{P}_{l_R}^{use})}. \quad (3)$$

Specifically, the power consumption for each link  $l$  in the route accounts for both the data transmission power  $P_{l_T}^{IT}$  for the corresponding transmitter

node  $l_T$  and the receive circuitry power  $\hat{P}_{l_R}^{use}$  for the corresponding receiver node  $l_R$ .

Our target problem aims to determine (1) a route for a source SN  $u_0$  to the gateway node  $g$ , (2) the transmit power of each SN in the route, and (3) the harvested power of each SN in the route, such that the NEE of the route is maximized. The target optimization problem can be formulated as

$$\begin{aligned}
& \underset{\mathbf{r}_{u_0,g}, \{P_{l_T}^{IT}\}}{\text{maximize}} && \Gamma_{u_0,g} \\
& \text{subject to:} && \\
& P_{l_T}^{IT} \leq \hat{B}_{l_T} + P_{out,l_T}^{DC\star}, && \forall l \in \mathbf{r}_{u_0,g}, \\
& P_{l_T}^{IT} \leq Q_{l_T}, && \forall l \in \mathbf{r}_{u_0,g}, \\
& R_l \geq R_{TH,l}, && \forall l \in \mathbf{r}_{u_0,g}.
\end{aligned} \tag{4}$$

The first constraint in the optimization problem limits the data transmission power  $P_{l_T}^{IT}$  of each link  $l$  to be within the power budget of the currently available battery power  $\hat{B}_{l_T}$  plus the power  $P_{out,l_T}^{DC\star}$  harvested from an ET cluster. Here,  $\hat{B}_{l_T}$  is defined as the difference between the remaining battery power  $B_{l_T}$  and the circuitry power consumption  $\hat{P}_{l_T}^{use}$ . The second constraint ensures that  $P_{l_T}^{IT}$  does not exceed the allowable interference threshold  $Q_{l_T}$  associated with link  $l$ , thus protecting the PN communication. The third constraint is a rate constraint, where  $R_{TH,l}$  is the minimum rate threshold for link  $l$ .

## 5. Solution Design

In this section, we provide a detailed description of each step of the proposed solution. The pseudocode for the solution algorithm can be found in Algorithm 1.

### 5.1. Route Determination

The framework of the proposed route determination (main loop) is described in the following. Let  $u_0$  be a source SN, and assume that the route from  $u_0$  to the  $k$ th SN  $u_k$  ( $k \geq 0$ ) has already been determined, i.e, the sequence  $(l_0, \dots, l_{k-1})$  of the route is given. The next step involves determining the  $(k+1)$ th SN  $u_{k+1}$  of the route among the set of neighboring SNs of  $u_k$ , denoted as  $\mathcal{S}_k$ , excluding the set  $\mathcal{Q}$  of SNs that have already been included in the route, in order to prevent loopbacks. We calculate the routing metric

$\chi[u]$  for all  $u \in \mathcal{S}_k$ . The next node  $u_{k+1}$  is then selected as the neighboring SN with the highest routing metric. This process is repeated until the gateway node is reached as the next node.

We develop two implementation methods within this framework: a centralized routing method (CRM) and a distributed routing method (DRM). In CRM, the source SN  $u_0$  determines the entire route to the gateway, denoted as  $\mathbf{r}_{u_0,g}$  (where the subscript  $g$  stands for the gateway). To adapt Problem (4) to CRM under the above framework, we convert the problem as follows:

$$\begin{aligned}
u_{k+1} &= \arg \max_{u \in \mathcal{S}_k - \mathcal{Q}} \chi[u] = \Gamma_{u_0,u}^* \\
&\text{subject to:} \\
\Gamma_{u_0,u}^* &= \max_{\{P_{l_T}^{IT}\}_{l \in \mathbf{r}_{u_0,u}}} \Gamma_{u_0,u}, u \in \mathcal{S}_k - \mathcal{Q} \\
P_{u_k}^{IT} &\leq \min\{\hat{B}_{u_k} + P_{out,u_k}^{DC*}, Q_{u_k}\}, R_{(u_k,u)} \geq R_{TH,(u_k,u)}.
\end{aligned} \tag{5}$$

The objective of this problem is to select  $u_{k+1}$  for given route up to  $u_k$ , which is executed in the main loop of the solution. For each candidate  $u$ , ET clustering (thus  $P_{out,u_k}^{DC*}$ ) and transmit power determination (thus obtaining  $\Gamma_{u_0,u}^*$ ) are associated. To calculate  $\Gamma_{u_0,u}$  and  $\Gamma_{u_0,u}^*$ , CRM requires full topology information of the WSN. We assume that a centralized database collects all the necessary information for implementing CRM, and each routing SN accesses it for routing purposes.

In contrast, DRM relies on each intermediate SN of a route to select the next routing SN. In DRM,  $u_k$  calculates the one-hop NEE from itself to a candidate node, i.e.,  $\Gamma_{u_k,u}, u \in \mathcal{S}_k$ , and selects  $u_{k+1}$  as the one achieving the highest one-hop NEE. Therefore, DRM only requires each SN to have information about neighboring SNs and does not require a centralized database. The DRM problem to be solved by each SN  $u_k, k = 0, \dots, K$  of a route is expressed as follows:

$$\begin{aligned}
u_{k+1} &= \arg \max_{u \in \mathcal{S}_k - \mathcal{Q}} \chi[u] = \Gamma_{u_k,u}^* \triangleq \frac{R_{(u_k,u)}}{P_{u_k}^{IT} + P_u^{use}} \\
&\text{subject to:} \\
\Gamma_{u_k,u}^* &= \max_{P_{(u_k,u)}^{IT}} \Gamma_{u_k,u}, u \in \mathcal{S}_k - \mathcal{Q}
\end{aligned} \tag{6}$$

with the same power and rate constraints as in (5).

We consider two benchmarks for centralized routing: (a) the centralized largest channel gain routing method (CLCGRM), and (b) the centralized

shortest distance routing method (CSDRM). For these two methods, the routing metrics are defined as the maximum total source-to-gateway routing channel gains ( $\chi[u_{k+1}] = \max_{u \in \mathcal{S}_{k-Q}} \sum_{l \in \mathbf{r}_{u_0, u}} h_l^{IT}$ ) and the minimum total source-to-gateway routing distances ( $\chi[u_{k+1}] = \min_{u \in \mathcal{S}_{k-Q}} \sum_{l \in \mathbf{r}_{u_0, u}} d_{u_k, u}$ ), respectively ( $d_{u_k, u}$  is the distance between  $u_k$  and  $u$ ). Similarly, we consider two counterpart benchmarks for distributed routing: (a) the distributed largest inter-node channel gain (DLCGRM,  $\chi[u_{k+1}] = \max_{u \in \mathcal{S}_{k-Q}} h_{(u_k, u)}^{IT}$ ), and (b) the distributed shortest inter-node distance (DSDRM,  $\chi[u_{k+1}] = \min_{u \in \mathcal{S}_{k-Q}} d_{u_k, u}$ ). The selected nodes in the benchmarks must meet the power and rate constraints.

## 5.2. ET Clustering

The harvested power  $P_{out, u}^{DC\star}$  of SN  $u$  in the power constraint of Problems (5) and (6) is determined by the ET clustering schemes described below and the utilized EH circuitry. Each ET employs maximum ratio transmission (MRT) for WPT to the EHNs associated with it ( $\mathcal{N}_x$  for ET  $x$ ). Consequently, ET  $x$  configures  $\{\mathbf{s}_{x, m}^{ET}\}_{m \in \mathcal{N}_x}$  as the column vectors of  $\sqrt{2P_x^{ET}} \frac{H_{\in \mathcal{N}_x}}{\|H_{\in \mathcal{N}_x}\|}$ , where  $H_{\in \mathcal{N}_x} = \{\mathbf{h}_{m, x}^{ET}\}_{m \in \mathcal{N}_x}$  consists of  $|\mathcal{N}_x|$  channels as matrix column vectors, satisfying  $\frac{1}{2} \sum_{m \in \mathcal{N}_x} \|\mathbf{s}_{x, m}^{ET}\|^2 \leq P_x^{ET}$  [26].

We develop two distinct clustering schemes for the ETs: harvested power-based clustering (HC) and channel gain-based clustering (CC). HC directly solves the problem of maximizing the power harvested by an EHN, which can be defined as

$$\underset{\mathcal{E}_m}{\text{maximize}} \quad \sum_{x \in \mathcal{E}_m} V_{out, m, x} \quad \text{such that } \mathcal{E}_m \subseteq \mathcal{E}. \quad (7)$$

The values of  $V_{out, m, x}$ ,  $x \in \mathcal{E}$  are first arranged in descending order as  $V_{out, m, x_1} \geq \dots \geq V_{out, m, x_i} \geq \dots \geq V_{out, m, x_{M_{ET}+1}}$ . Then, ET  $x_i$  from which the EHN can harvest power over a threshold  $\epsilon$  is included, i.e.,  $\mathcal{E}_m^{HC} = \{x_i | x_i \in \mathcal{E}, V_{out, m, x_i} > \epsilon\}$ . When  $V_{out, m, x_i}$  is accumulatively summed for increasing  $i = 1, 2, \dots$ , two possible outcomes can occur: (a) the sum saturates at a specific value  $i^*$  where the contribution of  $V_{out, m, x_j}$  for  $j > i^*$  to the sum becomes negligible, or (b) the sum continues to increase. For outcome (a), a group of ETs ( $x_1, \dots, x_{i^*}$ ) will transfer power to the EHN, while for outcome (b), all ETs will transfer power to the EHN.

In the CC scheme, an EHN forms a cluster of ETs with channel gains that are greater than the average channel gain of all ETs. This way, the EHN is

expected to receive stronger power signals from nearby ETs. Mathematically, the set of ETs in the CC cluster for EHN  $m$  is denoted by  $\mathcal{E}_m^{CC} = \{x|x \in \mathcal{E}, \|\mathbf{h}_{m,x}^{ET}\|^2 \geq \frac{1}{M^{ET}} \sum_{x \in \mathcal{E}} \|\mathbf{h}_{m,x}^{ET}\|^2\}$ .

In the evaluation, we compare the performance of the HC and CC schemes against a naive approach, wherein each EHN is served by all ETs (that is,  $\mathcal{E}_m^{AC} = \mathcal{E}$ ). We refer to this approach as all-ET clustering (AC).

### 5.3. Transmit Power Determination

To solve the transmit power optimization problem in (5) and (6), we use the Dinkelbach dual decomposition method [30] to convert the fractional objective function ( $\Gamma_{u,v}$ ) into a new function as follows:

$$V_{u,v} \triangleq \sum_{l \in \mathbf{r}_{u,v}} R_l(P_{l_T}^{IT}) - \lambda \left[ \sum_{l \in \mathbf{r}_{u,v}} (P_{l_T}^{IT} + \hat{P}_{l_R}^{use}) \right], \quad (8)$$

with a new variable  $\lambda$ . Then, the original problem is transformed into

$$\begin{aligned} & \text{maximize } V_{u,v} \text{ subject to:} \\ & \{P_{l_T}^{IT}\}_{l \in \mathbf{r}_{u,v}} \\ & \frac{2^{R_l} - 1}{g_l^{IT}} \leq P_{l_T}^{IT} \leq \min\{\hat{B}_{l_T} + P_{out,l_T}^{DC}, Q_{l_T}\}, \forall l \in \mathbf{r}_{u,v}, \end{aligned} \quad (9)$$

where  $g_l^{IT} = |h_l^{IT}|^2 / (\sum_{r=l_T, l' \in \mathcal{P}} |h_r^{NT}|^2 P_r^{IT} + \sigma^2)$ . The two constraints in (4) have been merged into a single constraint. Problem (9) is a convex optimization problem with respect to  $\{P_{l_T}^{IT}\}_{l \in \mathbf{r}_{u,v}}$ . Therefore, to find an optimal value for  $P_{l_T}^{IT}$  for a given  $\lambda$ , a line search can be used [30]. Specifically, the optimal value can be calculated as  $P_{l_T}^{IT*} = \min\{\bar{P}_{l_T}^{IT}, Q_{l_T}\} / \max_{n_T(l') \in \mathcal{P}} h_{n_T(l')}^{PT}$ , where  $\bar{P}_{l_T}^{IT}$  represents the solution obtained by the line search algorithm. Then,  $\lambda$  is updated to  $\sum_{l \in \mathbf{r}_{u,v}} R_l(P_{l_T}^{IT*}) / \left[ \sum_{l \in \mathbf{r}_{u,v}} (P_{l_T}^{IT*} + \hat{P}_{l_R}^{use}) \right]$ . Solving (9) and updating  $\lambda$  are repeated until convergence, after which  $\lambda$  is used as  $\Gamma_{u,v}^*$ .

## 6. Complexity and Signaling Overhead Analysis

This section presents an analysis of computational complexity and signaling overhead associated with the developed solution. A summary of the analysis is provided in Table 3.

---

**Algorithm 1** Solution algorithm.

---

```
1:  $\mathcal{Q}$ : A set of SNs included in a route
2: for given source SN  $u_0$  do
3:    $k \leftarrow 0$ ,  $\mathcal{Q} \leftarrow \{u_0\}$ ,  $\chi[u_{k+1}] \leftarrow 0$ 
4:   repeat
5:     for all  $u \in \mathcal{S}_k - \mathcal{Q}$  do
6:       Determine  $u$ 's ET cluster using HC, CC, or AC
7:       Calculate  $u$ 's harvested power as  $P_{out,u}^{DC}$ 
8:       Use  $P_{out,u}^{DC}$  for the routing power budget constraint
9:       Initialize  $\lambda$ 
10:      if CRM then
11:         $\hat{u} \leftarrow u_0$ 
12:      else if DRM then
13:         $\hat{u} \leftarrow u_k$ 
14:      end if
15:      repeat
16:        Find  $\{P_v^{IT^*}\}_{v=\hat{u}}^u$  using a line search method
17:        Update  $\lambda = \sum_{v=\hat{u}}^u R_i / [\sum_{v=\hat{u}}^u (\hat{P}_i^{use} + P_{i-1}^{IT^*})]$ 
18:      until  $V_{\hat{u},u}(\{P_v^{IT^*}\}_{v=\hat{u}}^u, \lambda)$  converges
19:       $\chi[u] \leftarrow \lambda$ 
20:      if  $\chi[u] > \chi[u_{k+1}]$  then
21:         $u_{k+1} \leftarrow u$ ,  $\chi[u_{k+1}] = \chi[u]$ 
22:      end if
23:    end for
24:    Add  $u_{k+1}$  to  $\mathcal{Q}$ ,  $k \leftarrow k + 1$ 
25:  until  $u_k$  is the gateway node
26:   $K \leftarrow k$ 
27:  Set the route as  $\{(u_0, u_1), \dots, (u_{K-1}, u_K)\}$ .
28: end for
```

---

### 6.1. Computational Complexity

Let  $\mathcal{O}(\mathcal{L}_p)$  and  $\mathcal{O}(\mathcal{A})$  represent the complexities associated with the power allocation iteration and non-iterative arithmetic operations, such as condition checks, variable value assignments, or primitive operations, respectively. In Algorithm 1, the complexities of the power allocation routine (Lines 15–18) for CRM and DRM are respectively given as  $A_{C1} = 3\mathcal{O}(I_p)K\hat{M}^{SN}$  and  $A_{D1} = 3\mathcal{O}(I_p)\hat{M}^{SN}$ . Here,  $3K\hat{M}^{SN}$  and  $3\hat{M}^{SN}$  represent the computational

Table 3: Comparison of computational complexity and signaling overhead between routing schemes

Method	Scheme	Node	Computational complexity	Transmission bits	CSI information	Node information
Centralized	CRM	Source	$A_{C1} + A_{C2} + \{A_{HC}/A_{CC}/A_{AC}\}$	$(K - k)i_0 + F$	Global CSIs	Global information
		Sensor	–	$(K - k)i_0 + F$	–	–
	CLCGRM	Source	$A_{A1} + A_{C2} + \{A_{HC}/A_{CC}/A_{AC}\}$	$(K - k)i_0 + F$	Global CSIs	Global information
		Sensor	–	$(K - k)i_0 + F$	–	–
	CSDRM	Source	$A_{A1} + A_{C2} + \{A_{HC}/A_{CC}/A_{AC}\}$	$(K - k)i_0 + F$	Global CSIs	Global information
		Sensor	–	$(K - k)i_0 + F$	–	–
Distributed	DRM	Source	$A_{D1} + A_{D2} + \{A_{HC}/A_{CC}/A_{AC}\}$	$i_0 + F$	Local CSIs	Local information
		Sensor	$A_{D1} + A_{D2} + \{A_{HC}/A_{CC}/A_{AC}\}$	$i_0 + F$	Local CSIs	Local information
	DLCGRM	Source	$A_{A2} + A_{D2} + \{A_{HC}/A_{CC}/A_{AC}\}$	$i_0 + F$	Local CSIs	Local information
		Sensor	$A_{A2} + A_{D2} + \{A_{HC}/A_{CC}/A_{AC}\}$	$i_0 + F$	Local CSIs	Local information
	DSDRM	Source	$A_{A2} + A_{D2} + \{A_{HC}/A_{CC}/A_{AC}\}$	$i_0 + F$	Local CSIs	Local information
		Sensor	$A_{A2} + A_{D2} + \{A_{HC}/A_{CC}/A_{AC}\}$	$i_0 + F$	Local CSIs	Local information

complexity of calculating  $\{P_v^{IT}\}_{v=\hat{u}}^u$ ,  $\lambda$  and  $V_{u,\hat{u}}$  imposed on a computing node for CRM and DRM, respectively ( $\hat{M}^{SN}$  is the expected number of neighboring SNs). The complexities of CLCGRM/CSDRM and DLCGRM/DSDRM are deduced as  $A_{A1} = \mathcal{O}(\mathcal{A})K\hat{M}^{SN}$  and  $A_{A2} = \mathcal{O}(\mathcal{A})\hat{M}^{SN}$ , respectively. It is noted that  $\mathcal{O}(I_p) > \mathcal{O}(\mathcal{A})$  since the power allocation of CRM and DRM involves iterative operations. Additionally, the other decision making (branching) and arithmetic operation complexity of Algorithm 1 can be expressed as  $A_{C2} = 6\mathcal{O}(\mathcal{A})K\hat{M}^{SN}$  and  $A_{D2} = 6\mathcal{O}(\mathcal{A})\hat{M}^{SN}$ . The first if statement (Lines 10–14) consists of only one operation ( $\mathcal{O}(\mathcal{A})$ ), while the second if statement (Lines 20–22) along with remaining operations (Line 19) consists of three operational components ( $3\mathcal{O}(\mathcal{A})$ ). Finally, the routing node set update and the routing nodes counter update (Line 24) are necessary, corresponding to the complexity of  $2\mathcal{O}(\mathcal{A})$ .

Regarding the ET clustering part (Line 6) of Algorithm 1, the complexities of HC, CC and AC are given as  $A_{HC} = 5\mathcal{O}(\mathcal{A})M^{ET}(M^{PL} + M^{SN})$ ,  $A_{CC} = \mathcal{O}(\mathcal{A})(M^{ET} + 2(M^{PL} + M^{SN}))$  and  $A_{AC} = 0$ , respectively. In this context, HC consists of the ordering and saturation point decision-making operations ( $2\mathcal{O}(\mathcal{A})$ ), as well as the MRT-based power allocation, harvested power calculation and the power summation operations ( $3\mathcal{O}(\mathcal{A})$ ) for every pair of EHNs and ETs. The CC scheme involves averaging channel gains and one decision-making operation based on the averaged channel gains ( $2\mathcal{O}(\mathcal{A})$ ), along with MRT-based ET power allocation for each ET ( $\mathcal{O}(\mathcal{A})$ ). The AC scheme requires no computation since ETs transmit to all EHNs.

The computational complexities of different schemes for executing Algorithm 1 are provided in Table 3. It can be observed that CRM requires more computation than CLCGRM and CSDRM due to the power allocation iteration. Similarly, DRM involves more computation at each node compared

to DLCGRM and DSDRM, also due to the power allocation iteration. The computational complexity of the centralized methods is focused on a source node while the complexity of the distributed methods is distributed among SNs along a route. Furthermore, the complexity of HC is higher than CC due to the maximization of harved power for combinations of EHNs and ETS, as indicated by the multiplication operation in  $A_{HC}$ .

### 6.2. Signaling Overhead Analysis

In the implementation of the centralized methods, the source node of the secondary WSN requires detailed information about inter-node channel gains, power requirements, the current available power for each SN, the interfering signals within the network, and the interference constraints set by the PN for all potential SNs on a route. This information can be stored in a centralized database and obtained by the source node through a wide-area broadcast from the gateway or via multi-hop communication, enabling the implementation of centralized schemes such as CRM, CLCGRM, and CS DRM. In contrast, the distributed schemes (DRM, DLCGRM, DSDRM) rely on the currently chosen routing node to possess such information for its neighboring nodes. To enable this, each node can broadcast its own information and listen to the information from neighboring nodes.

During each packet transmission in the centralized methods, the current node transmits the indexes of subsequent routing nodes and the information bits ( $F$ ). The total number of bits transmitted from the current node can be calculated as  $(K - k)i_0 + F$ , where  $K$  represents the total number of selected routing nodes,  $k$  denotes the current routing node number, and  $i_0$  is the required number of bits to represent a node index. In the distributed methods, the current routing node transmits both the information bits and the index of the selected next routing node, resulting in a total transmission of  $i_0 + F$  bits.

## 7. Performance Evaluation

We present the numerical evaluation results in this section. The nodes of the PN, WSN, and ETs are randomly distributed within a 1000m×1000m field, as illustrated in Fig. 4. The inter-node channel model is given as  $h = \sqrt{C_0(c/4\pi fd)^\alpha G_t G_r} \tilde{h}$ , where  $C_0 = 10$  dB is the transmitted signal attenuation coefficient at a reference distance of 1m;  $c = 3 \times 10^8$  m/s,  $f([f_P, f_I] =$

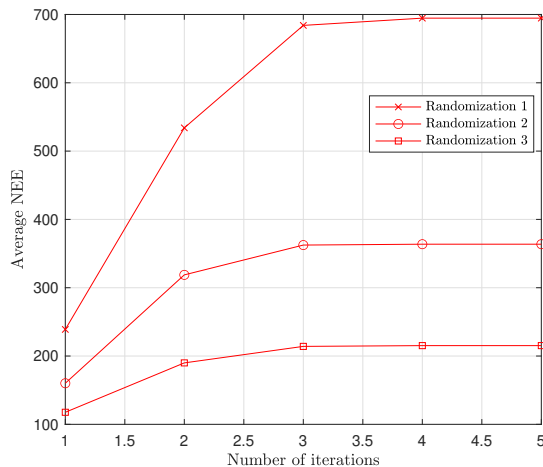


Figure 2: Illustration of the convergence of Algorithm 1 for different randomization cases of node placement.

[5.18, 2.4]GHz),  $G_t = 6$  dBi,  $G_r = 6$  dBi are the speed of light, the transmitting device carrier frequency, the transmitter and receiver antenna gains, respectively;  $\alpha = 3$  is a pathloss exponent, and  $d$  is the distance between transmitting and receiving nodes;  $\tilde{h}$  is a small-scale fading factor with a Rayleigh distribution, having zero mean and a variance of one. We set the following parameters for the simulations:  $R_{ant,m} = 50 \Omega$ ,  $R_{Lod,m} = 100 \text{ k}\Omega$ ,  $\eta_m = 1.05$ , and  $V_{T,m} = 25.86 \text{ mV}$ . Other simulation parameters include the range of SN battery power ( $-10 \leq B_k \leq 30$ ) dBm, noise power ( $-175 \text{ dBm/Hz}$ ), bandwidth (3 MHz),  $M^{SN} = 200$ ,  $M^{PL} = 100$ ,  $10 \leq M^{ET} \leq 50$ ,  $10 \leq N_x^{ET} \leq 20$ ,  $G_m = 4$ ,  $P_r^{PT} = -5 \text{ dBm}$ ,  $\hat{P}_k^{use} = -15 \text{ dBm}$ , and  $R_{TH,k} = 0.1375 \text{ bps/Hz}$  (for the SNR of  $-10 \text{ dB}$ ). Each figure was obtained from  $10^4$  channel randomization.

Figs. 2 and 3 illustrate the convergence of Algorithm 1 and the concave nature of the  $V_{u,v}$  function with respect to  $P_{l_T}^{IT}$ , respectively. These figures present the results for different randomization cases of node placement, while other parameters remain as previously specified. In Fig. 2, it can be observed that the proposed routing algorithm converges in fewer than five iterations, regardless of the node placement. This indicates that the algorithm effectively achieves convergence under various inter-node transmission conditions. Fig. 3 shows that  $V_{u,v}$  exhibits concavity with respect to  $P_{l_T}^{IT}$ , as discussed in the transmit power determination solution, across different node placement

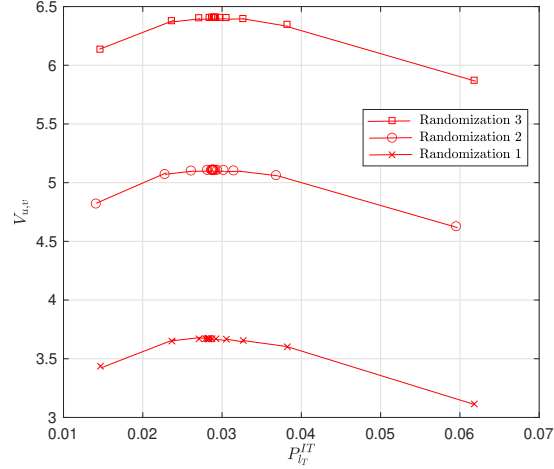


Figure 3: Illustration of the concavity of  $V_{u,v}$  with respect to  $P_{l_T}^{IT}$  for different randomization cases of node placement.

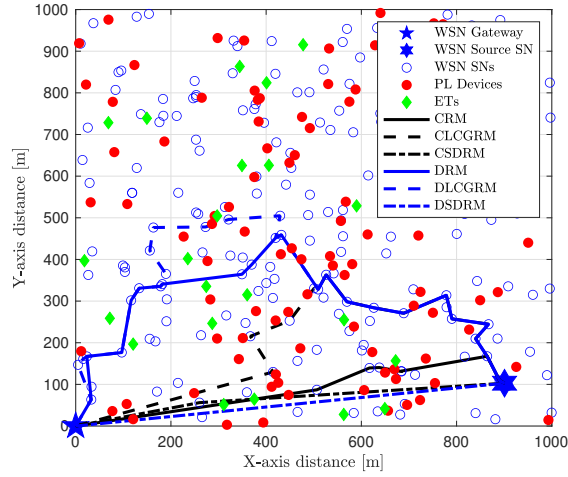


Figure 4: Illustration of routing results.

scenarios. This indicates that the optimal  $P_{l_T}^{IT}$  can be determined using an unconstrained line search method. The Golden search method was employed throughout the simulation, including in Fig. 3.

Fig. 4 illustrates the routes determined by various methods between a gateway located at  $(0, 0)$  and a source SN at  $(900, 100)$ . The shortest distance methods (CSDRM and DSDRM) tend to use the fewest hops, fol-

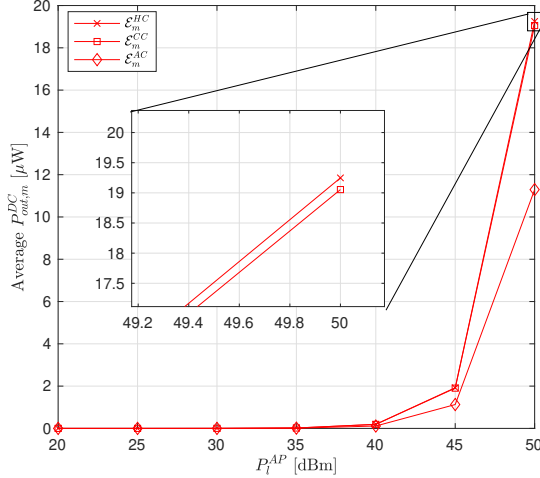


Figure 5: Average harvested power ( $P_{out,m}^{DC}$ ) for increasing ET power  $P_l^{ET}$ .

lowed by CRM and then CLGGRM. The remaining two distributed methods (DRM and DLCGRM) exhibit the longest routes. However, subsequent results demonstrate that the NEE achieved by a routing scheme is influenced not only by the length of the determined route but also by other factors. For instance, CS DRM and DS DRM, the two schemes utilizing the fewest hops, achieve lower NEE values compared to the other schemes, as will be demonstrated in the following analysis.

Fig. 5 shows the amount of power harvested by each EHN as the ET power ( $P_l^{ET}$ ) increases. The two proposed clustering schemes (HC and CC) exhibit similar harvesting performance to the benchmark scheme (AC) for  $P_l^{ET} < 40$  dBm. However, for  $P_l^{ET} > 40$  dBm, HC and CC outperform AC by harvesting an additional  $8 \mu W$  power at  $P_l^{ET} = 50$  dBm. This occurs because the ET power resource is shared among multiple EHNs; as the number of EHNs associated with an ET increases, the ET power allocated to each EHN decreases. In the following analysis, routing schemes are evaluated using the HC clustering scheme.

The impact of the PTs transmit power and interference constraints on WSN performance is shown in Figs. 6 and 7. These figures contain subplots of (a) average NEE, (b) the number of routing SNs for a route ( $K$ ), (c) each SN's average achievable rate ( $R_k$ ), and (d) each SN's average transmit power ( $P_k^{IT}$ ). In both figures, the descending performance of various schemes

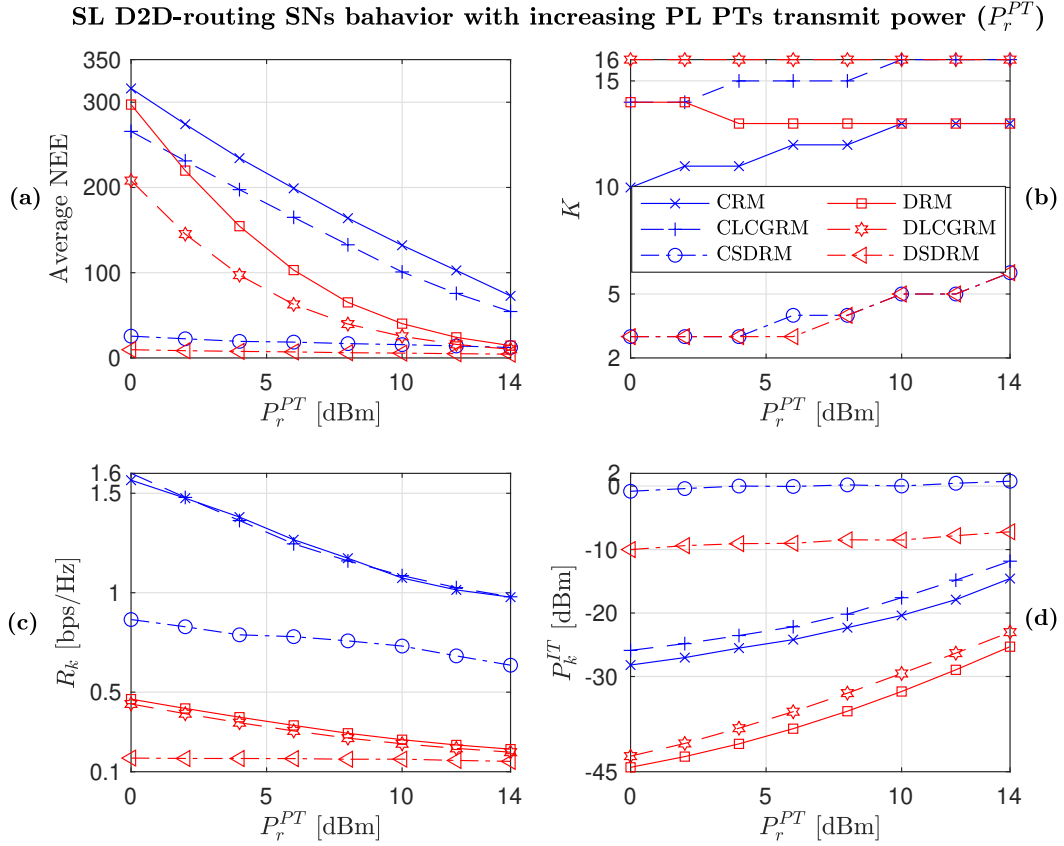


Figure 6: Impact of PT transmit power  $P_r^{PT}$  on WSN performance.

for NEE,  $R_k$  and  $P_k^{IT}$  are CRM, CLCGRM, DRM, DLCGRM, CSDRM and then DSDRM. The NEE decreases for all routing schemes with increasing  $P_r^{PT}$ , as observed in Fig. 6(a). This is due to the PTs' interference with the WSN, leading to a reduction in achievable rates ( $R_k$ ), as shown in Fig. 6(c). However, as  $P_r^{PT}$  increases, the  $P_k^{IT}$  also rises, as depicted in Fig. 6(d), to enhance the SNs' achievable rate  $R_k$ . The reduction in NEE is also due to the increasing number of SNs used in the routing, as seen in Fig. 6(b), which leads to an increase in  $P_k^{IT}$ . However, DRM and DLCGRM mostly exhibit constant  $K$  due to the utilization of individual inter-node NEE and channel gains. Fig. 7 demonstrates similar behavior for different interference constraint values. The NEE decreases for all schemes with increasing interference constraint, while  $R_k$  and  $P_k^{IT}$  decrease and increase, respectively, as

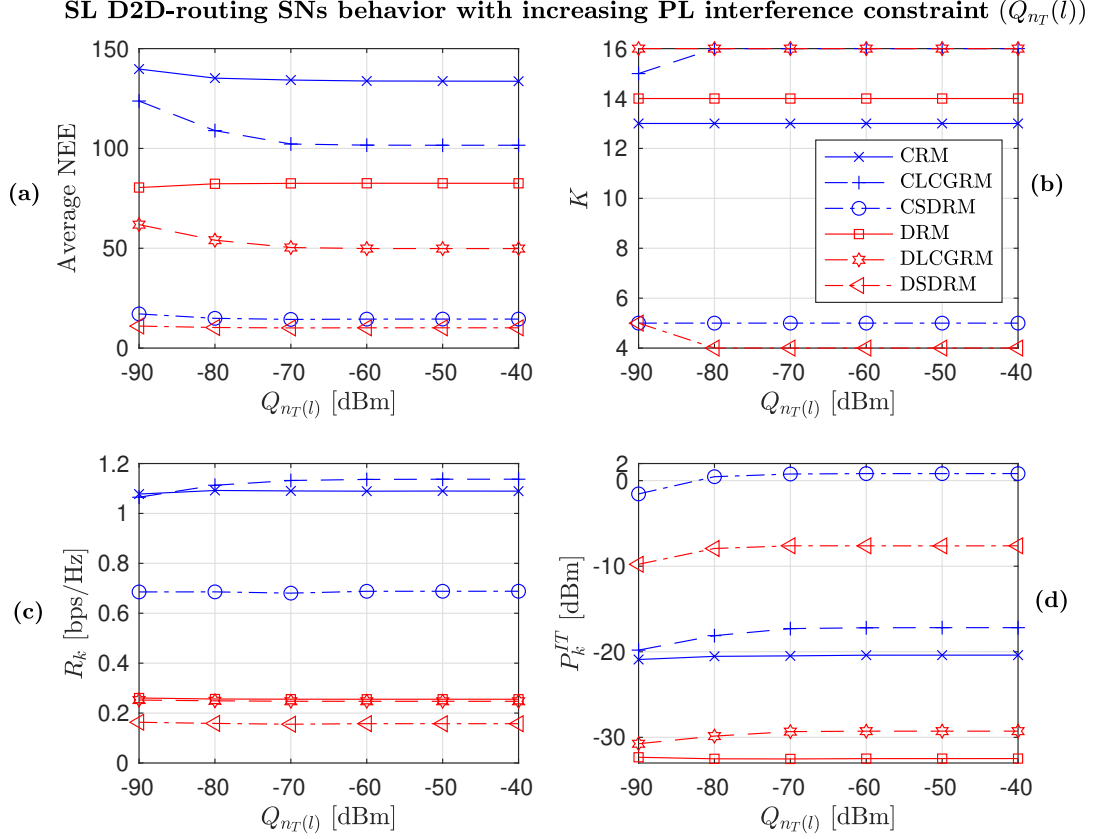


Figure 7: Impact of PN interference constraint  $Q_{n_T(l)}$  on WSN performance.

expected.

In summary, the results indicate that the proposed CRM consistently outperforms not only its distributed counterpart (DRM) but also other benchmarks across the considered range of system parameters. Despite the substantial performance gap between CRM and DRM, DRM surpasses the distributed benchmarks and even the centralized benchmark CSDRM, while offering the advantage of not necessitating a central database or the collection of topology information.

## 8. Conclusion

In this study, we investigated a spectrum-sharing network composed of PLs and a WSN, which is aided by EH. We proposed an integrated approach

for addressing routing, transmit power determination, and ET clustering. The approach encompasses both centralized and distributed routing schemes, along with two ET clustering schemes. The simulation results demonstrated that our proposed solution and associated schemes surpass their respective benchmark methods in performance.

There are several areas that warrant further exploration in future work. These include investigating single-band symbiotic cognitive radio network approaches, exploring different WPT techniques, including SWIPT, and integrating advanced multiple access transmission schemes.

## References

- [1] F. S. Shaikh, R. Wismüller, Routing in multi-hop cellular device-to-device (D2D) networks: A survey, *IEEE Commun. Surveys & Tutorials* 20 (4) (2018) 2622–2657.
- [2] T. Van Nguyen, T.-N. Do, V. N. Q. Bao, D. B. da Costa, B. An, On the performance of multi-hop cognitive wireless powered D2D communications in WSNs, *IEEE Trans. Veh. Technol.* 69 (3) (2020) 2684–2699.
- [3] Q. Ren, G. Yao, An opportunistic routing for energy-harvesting wireless sensor networks with dynamic transmission power and duty cycle, *IEEE Access* 10 (2022) 121109–121119.
- [4] D. K. P. Asiedu, H. Lee, K.-J. Lee, Simultaneous wireless information and power transfer for decode-and-forward multihop relay systems in energy-constrained IoT networks, *IEEE Internet of Things J.* 6 (6) (2019) 9413–9426.
- [5] H. Xiao, H. Jiang, L.-P. Deng, Y. Luo, Q.-Y. Zhang, Outage energy efficiency maximization for UAV-assisted energy harvesting cognitive radio networks, *IEEE Sensors J.* 22 (7) (2022) 7094–7105.
- [6] A. Omidkar, A. Khalili, H. H. Nguyen, H. Shafiei, Reinforcement-learning-based resource allocation for energy-harvesting-aided D2D communications in IoT networks, *IEEE Internet Things J.* 9 (17) (2022) 16521–16531.

- [7] H. Xiao, C. Wu, H. Jiang, L.-P. Deng, Y. Luo, Q.-Y. Zhang, Energy-efficient resource allocation in multiple uavs-assisted energy harvesting-powered two-hop cognitive radio network, *IEEE Sensors J.* 23 (7) (2023) 7644–7655.
- [8] S. He, Y. Tang, Z. Li, F. Li, K. Xie, H.-j. Kim, G.-j. Kim, Interference-aware routing for difficult wireless sensor network environment with SWIPT, *Sensors* 19 (18) (2019) 3978.
- [9] M. M. Salim, H. A. Elsayed, M. Abd Elaziz, M. M. Fouda, M. S. Abdalzaher, An optimal balanced energy harvesting algorithm for maximizing two-way relaying d2d communication data rate, *IEEE Access* 10 (2022) 114178–114191.
- [10] S. Aslam, M. Ibnkahla, Optimized node classification and channel pairing scheme for RF energy harvesting based cognitive radio sensor networks, in: *IProc. IEEE 12th Int. Multi-Conf. Syst. Signals Devices (SSD15)*, 2015, pp. 1–6.
- [11] W. E. S. Aslam, M. Ibnkahla, Energy and spectral efficient cognitive radio sensor networks for internet of things, *IEEE Internet Things J.* 5 (4) (2018) 3220–3233.
- [12] J. Wang, H. Yu, RF energy harvesting schemes for intelligent reflecting surface-aided cognitive radio sensor networks, *Scientific Reports* 2 (22462) (2022) 1–13.
- [13] Y. Y. Z. Liu, M. Zhao, X. Guan, Subchannel and resource allocation in cognitive radio sensor network with wireless energy harvesting, *Comput. Netw.* 167 (2020) 1–10.
- [14] J. Wang, Y. Ge, A radio frequency energy harvesting-based multihop clustering routing protocol for cognitive radio sensor networks, *IEEE Sensors Journal* 22 (7) (2022) 7142–7156.
- [15] J. Wang, Y. Ge, An energy balance-oriented clustering routing protocol for cognitive radio sensor networks, *IEEE Sensors Journal* 22 (21) (2022) 21035–21048.

- [16] J. Wang, C. Li, A weighted energy consumption minimization-based multi-hop uneven clustering routing protocol for cognitive radio sensor networks, *Scientific Reports* 12 (14039) (2022) 1–16.
- [17] J. Wang, C. Liu, An imperfect spectrum sensing-based multi-hop clustering routing protocol for cognitive radio sensor networks, *Scientific Reports* 13 (4853) (2023) 1–16.
- [18] D. L. Galappaththige, R. Shrestha, G. A. A. Baduge, Exploiting cell-free massive MIMO for enabling simultaneous wireless information and power transfer, *IEEE Trans. on Green Commun. and Netw.* 5 (3) (2020) 1541 – 1557.
- [19] X. Wang, A. Ashikhmin, X. Wang, Wirelessly powered cell-free IoT: Analysis and optimization, *IEEE Internet Things J.* (2020) 8384 – 8396.
- [20] T. N. Tran, T. Van Nguyen, V. N. Q. Bao, B. An, An energy efficiency cluster-based multihop routing protocol in wireless sensor networks, in: *in Proc. Int. Conf. Advanced Technol. Commun.*, IEEE, 2018, pp. 349–353.
- [21] S. He, K. Xie, W. Chen, D. Zhang, J. Wen, Energy-aware routing for SWIPT in multi-hop energy-constrained wireless network, *IEEE Access* 6 (2018) 17996–18008.
- [22] S. Hao, Y. Hong, Y. He, An energy-efficient routing algorithm based on greedy strategy for energy harvesting wireless sensor networks, *Sensors* 22 (4) (2022) 1–24.
- [23] B. Han, F. Ran, J. Li, L. Yan, H. Shen, A. Li, A novel adaptive cluster based routing protocol for energy-harvesting wireless sensor networks, *Sensors* 22 (4) (2022) 1–16.
- [24] W. Kim, M. M. Umar, S. Khan, M. A. Khan, Novel scoring for energy-efficient routing in multi-sensored networks, *Sensors* 22 (4) (2022) 1–21.
- [25] N. Subramani, P. Mohan, Y. Alotaibi, S. Alghamdi, O. I. Khalaf, An efficient metaheuristic-based clustering with routing protocol for underwater wireless sensor networks, *Sensors* 22 (2) (2022) 1–16.

- [26] S. Shen, B. Clerckx, Beamforming optimization for MIMO wireless power transfer with nonlinear energy harvesting: RF combining versus DC combining, *IEEE Trans. Wireless Commun.* 20 (2020) 199–213.
- [27] Z. Jiang, Z. Wang, M. Leach, E. G. Lim, H. Zhang, R. Pei, Y. Huang, Symbol-splitting-based simultaneous wireless information and power transfer system for WPCN applications, *IEEE Microw. and Wireless Compon. Lett.* 30 (7) (2020) 713–716.
- [28] M. Wagih, G. S. Hilton, A. S. Weddell, S. Beeby, Dual-band dual-mode textile antenna/rectenna for simultaneous wireless information and power transfer (SWIPT), *IEEE Trans. Antennas Propag.* 69 (2021) 6322 – 6332.
- [29] B. Clerckx, Wireless information and power transfer: Non-linearity, waveform design, and rate-energy tradeoff, *IEEE Trans. Signal Process.* 66 (4) (2017) 847–862.
- [30] H. Tuy, *Convex analysis and global optimization*, Springer Science & Business Media (1998).